Optical Engineering

OpticalEngineering.SPIEDigitalLibrary.org

Modeling macular pigment optical density effects on photopic and scotopic vision in degraded visual environments

Kevin J. O'Brien
Leonard A. Temme
Paul M. St. Onge

SPIE.

Kevin J. O'Brien, Leonard A. Temme, Paul M. St. Onge, "Modeling macular pigment optical density effects on photopic and scotopic vision in degraded visual environments," *Opt. Eng.* **58**(5), 051805 (2018), doi: 10.1117/1.OE.58.5.051805.

Modeling macular pigment optical density effects on photopic and scotopic vision in degraded visual environments

Kevin J. O'Brien,[a,b,*] Leonard A. Temme,[a] and Paul M. St. Onge[a,c]
[a]U.S. Army Aeromedical Research Laboratory, Fort Rucker, Alabama, United States
[b]Oak Ridge Institute for Science and Education, Oak Ridge, Tennessee, United States
[c]Laulima Government Solutions, LLC, Orlando, Florida, United States

Abstract. The macular pigment (MP) is an accumulation of the carotenoids lutein, zeaxanthin, and mesozeaxanthin in the central retina. These are derived from dietary sources. MP absorbs light in the 400- to 520-nm range. Consequently, the MP is a spectral filter over the photoreceptors, reducing the effects of internally scattered light and attenuating the short wavelength component of natural sunlight. The average MP optical density (OD) is about 0.2 to 0.6 log units depending on the sample population, whereas the range of MPOD is reportedly 0 to 1.5 log units. Some people can increase their MPOD by increasing their consumption of lutein, zeaxanthin, and mesozeaxanthin, and this may be important for vision in degraded visual environments (DVE). Specifically, nutritional interventions and dietary supplements have produced statistically significant enhancements under laboratory conditions in visual tasks, such as visibility through haze, low contrast target detection, contrast sensitivity, glare resistance and recovery, photostress recovery, dark adaptation, mesopic sensitivity, and enhanced reaction times. The question is whether these enhancements are operationally meaningful or not. The present paper begins to address the question by modeling MPOD effects on the visibility to low contrast photopic and scotopic targets seen under a range of DVE over realistic distances that incorporate atmospheric filtering. Specific model parameters include luminance, target contrast, spectral content, and distance. The model can be extended to estimate the efficacy of MPOD effects on target detection, discrimination, and standoff distances.
 [DOI: 10.1117/1.OE.58.5.051805]

Keywords: macular pigment; visibility; degraded visual environment; photopic; scotopic; Weber contrast.

Paper 181249SS received Aug. 29, 2018; accepted for publication Nov. 28, 2018; published online Dec. 27, 2018.

1 Introduction

Research and development of countermeasures for degraded visual environments (DVEs) commonly focuses on technologic solutions to transient ambient conditions. This approach typically views "degraded visuals" as an intrinsic characteristic of the environment, separated from the human operator. When examining human factors in DVEs, it may be helpful to reframe the situation as one in which the operator's "visual environment" has been degraded. Everything which occurs prior to transduction of photons into neural signals by the photoreceptors contributes to an operator's "visual environment," but much of this is not captured in the technology-centric DVE mitigation framework.

Aviation may be one of the fields most broadly interested in DVE, due to safety and performance implications. With the common approach, the "E" portion of DVE is typically everything outside of the cockpit, including changes in lighting, fog, sand, smoke, and dust, which contribute to the "DV" portion. The pilot's visual environment not only includes the outside world, but the windshield, any obstructions to the windshield, the interior of the cockpit, any worn filters (such as sunglasses), the pilot's refractive elements (i.e., corrective eyewear, the cornea, and the crystalline lens), the aqueous and vitreous humors (including any debris present), and the macular pigment (MP).

*Address all correspondence to Kevin J. O'Brien, E-mail: kevin.j.obrien99.civ@mail.mil

The MP is composed of carotenoids (specifically lutein, zeaxanthin, and mesozeaxanthin[1]) derived from dietary sources and deposited in multiple layers through the macula, the part of the retina that supports central vision. The MP is in the optical path between the vitreous humor and the photoreceptors and serves as a filter, attenuating shorter wavelengths in the visible spectrum while allowing longer wavelengths to pass through. Although this has many potential implications for DVE (such as reducing glare disability), of particular interest to the modeling effort described in this paper is the filtering of the short-wave components of light scattered in the atmosphere when viewing distant objects.

When viewing distant objects through the atmosphere, light is scattered by the molecules and particles in the viewing path. Smaller particles tend to cause Rayleigh scattering,[2] which is strongly wavelength dependent (with shorter wavelengths scattering more than longer wavelengths), and larger particles tend to cause Mie scattering,[3] which is largely wavelength independent. As a result, the scattered light between a viewer and a distant object is somewhere between strongly shortwave predominant (such as at high elevations with clear skies) and spectrally flat (such as in extreme fog) depending on local atmospheric conditions. This short-wave scattering, combined with the short-wave filtration of MP, is of particular relevance to the model presented here.

Wooten and Hammond[4] proposed that MP would improve contrast for objects at long ranges by removing some of the scattered shortwave light (referred to as "airlight") intruding between the observer and target, and the

shortwave component of the background while largely preserving the wavelengths of the target. The rationale they presented for their model is reasonable, but due to technological constraints at the time of their work, the model incorporated simplifying assumptions to reduce computational complexity, assumptions that may have important implications for their conclusions. Examining this situation is of more than theoretical interest as the optical density of the macular pigment (MPOD) in the normal human eye can vary widely between individuals. Moreover, a growing robust literature shows that the MPOD in humans can be substantially affected by diet and dietary supplementation. Thus, the model provides one way to evaluate the impact that differences in MPOD between and within individuals may have on an important aspect of visual performance in DVE. The present paper documents an elaborated, refined, and updated version of the Wooten and Hammond[4] model. The results reported here extend an earlier report of our instantiation of the model that demonstrated the feasibility of using the model to estimate the impact of MPOD changes on human performance in DVE under photopic conditions. Refinements in the modeling allowed greater resolution in characterizing the effects of MPOD on photopic vision and improvements made it possible to characterize MPOD's effects under scotopic conditions, which to our knowledge has not previously been reported.

2 Methods

The model specifically evaluates the effects of MPOD on Weber contrast (WC). WC is the standard measurement of contrast between an object and its background when the ratio of the angular area of the background to the angular area of the object is high. The model incorporates the impact of distance, luminance, and spectra on WC. As the distance between an object and an observer increases, shorter wavelengths of light will be lost to a greater degree than longer wavelengths due to wavelength-dependent Rayleigh scattering.[5,6] This is captured in the exponential term of equation 1 (below). Additionally, as the distance of a viewed object increases, more light (which also exhibits the same wavelength-dependent scattering) is present in the air of the viewing path. This intruded light is identified as the target airlight luminance. The Wooten and Hammond[4] model treats the horizon sky luminance as the background luminance for calculating the contrast of an object against an open sky. The addition of a term incorporating atmospheric scattering produces the airlight luminance equation. The model presented here treats the background luminance as an extreme-distance case of the airlight luminance. In the presented results, the difference between these two is negligible, as the exponent term approaches values extreme enough to drive the multiplier toward 1. In other applications if the atmospheric scatter constant is sufficiently small (e.g., due to extreme fog) then this multiplier may not be 1 in which case the effective background distance may have a significant impact. For this reason, it is incorporated into the model for future use, but does not currently meaningfully contribute to the results.

1. $\text{Luminance}_{\text{target}} = \int_{0.400\ \mu\text{m}}^{0.700\ \mu\text{m}} V_\lambda E_\lambda a_\lambda \frac{T_{\lambda,\text{mod}}}{T_{\lambda,\text{avg}}} e^{-c(\lambda^{-v})R} \text{d}\lambda$
2. $\text{Luminance}_{\text{target airlight}} = \int_{0.400\ \mu\text{m}}^{0.700\ \mu\text{m}} V_\lambda E_\lambda \frac{T_{\lambda,\text{mod}}}{T_{\lambda,\text{avg}}} 1 - e^{-c(\lambda^{-v})R} \text{d}\lambda$
3. $\text{Luminance}_{\text{horizon sky}} = \int_{0.400\ \mu\text{m}}^{0.700\ \mu\text{m}} V_\lambda E_\lambda \frac{T_{\lambda,\text{mod}}}{T_{\lambda,\text{avg}}} \text{d}\lambda$
4. $\text{Luminance}_{\text{background}} = \int_{0.400\ \mu\text{m}}^{0.700\ \mu\text{m}} V_\lambda E_\lambda \frac{T_{\lambda,\text{mod}}}{T_{\lambda,\text{avg}}} 1 - e^{-c(\lambda^{-v})R_{ex}} \text{d}\lambda \approx \text{Luminance}_{\text{horizon sky}}$
5. $\text{Weber Contrast} = \frac{(\text{Luminance}_{\text{target}} + \text{Luminance}_{\text{target airlight}}) - \text{Luminance}_{\text{background}}}{\text{Luminance}_{\text{background}}}$

Table 1 Terms for equations.

Variable	Description	Source
V_λ	Luminosity function (Photopic 2006 CIE or Scotopic 1951 CIE)	CVRL.org[7]
E_λ	Illuminant spectrum (D65)	CVRL.org[7]
a_λ	Target reflectance spectrum	USGS Spectral Library[8]
$T_{\lambda,\text{mod}}$	Transmittance of MP matching modeled observer density	Calculated from tabular data retrieved from CVRL.org[7]
$T_{\lambda,\text{avg}}$	Transmittance of MP matching assumed observers used to generate luminosity functions	Calculated from tabular data retrieved from CVRL.org[7]
c	A constant assumed to be $0.1/(0.55^{-2})$	Back-calculated from Wooten and Hammond[4]
λ	Wavelength (in μm)	(Present in tabular data)
v	Atmospheric scatter constant between 0.00 and 4.00	Sequenced for model
R	Range in kilometers	Sequenced for model
R_{ex}	An extreme range (in this case 1000 km) which, when inserted into the target airlight luminance term, asymptotically approaches the horizon sky term described in the previous presentation[9] but incorporates the atmospheric scatter constant for future use in DVE modeling	Selected as 1000 km to push exponential term toward asymptote, but may be specified as other ranges in future applications

For all calculations, λ (Table 1) was 1-nm bins ranging from 400 to 700 nm, for a total of 301 wavelengths. $T_{\lambda,\mathrm{mod}}$ for each wavelength was calculated for 101 possible optical densities (0.00 to 1.00 in increments of 0.01). The λ^{-v} term for each wavelength was calculated for each of 401 possible atmospheric scatter coefficients (0.00 to 4.00 in increments of 0.01). For any combination of V, E, a, and $T_{\lambda,\mathrm{avg}}$, this represents ~12.19 million calculations each for target, airlight, and background luminance prior to distance being incorporated. Target luminance, target airlight luminance, and background luminance were calculated for each wavelength for every combination of viewing distance, MPOD, and atmospheric scatter coefficient. In the previous presentation of this approach, the integral approximation was performed using the trapezoidal method. Due to the small width of the λ bins and their quantity, this step was replaced by taking the bins as an array along with an equivalent length array of ones and calculating the dot product (i.e., "scalar product"). This significantly reduced run-time, and in cursory testing was not found to significantly alter luminance calculations.

Tested spectra included that of an ideal black body (i.e., a target with no reflectance whatsoever), olive drab green nylon webbing, and yellow nylon webbing. These two nylon samples were chosen because they were among the few synthetic materials with spectra available from the USGS (U.S. Geological Survey), which appear with multiple pigments but identical base materials and are potentially found in a military environment. The D65 standard illuminant was used for the E_λ term and the luminosity functions used were the 2006 CIE (International Commission on Illumination) Photopic data and the 1951 CIE Scotopic data. Due to the a lack of other suitable values to assume, the $T_{\lambda,\mathrm{avg}}$ term used corresponded to a zero MPOD observer. It is worth noting that this brings the associated denominator term for all wavelengths to 1 by assuming no filtration from the MP occurs. The $T_{\lambda,\mathrm{mod}}$ term was calculated by multiplying the normalized absorption spectra for MP by the absorption corresponding to each modeled MPOD, then converting from absorption to transmittance (Fig. 1).

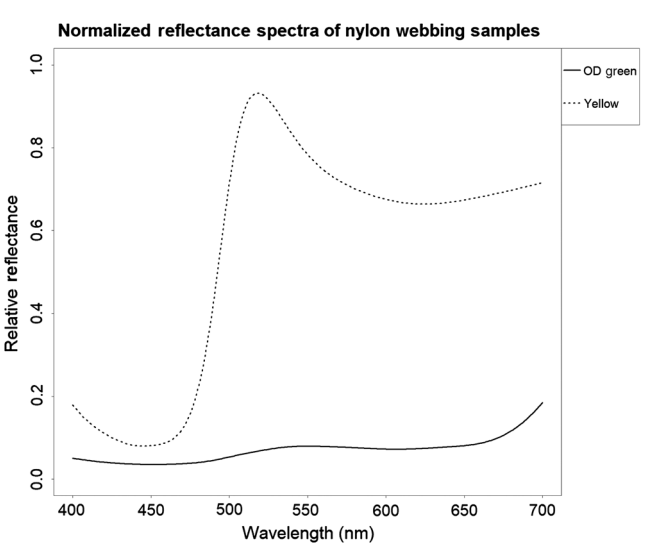

Fig. 1 Reflectance spectra of OD green and yellow nylon webbing samples.

For each spectra, contrasts were calculated for 100 ranges (500 m to 50 km in 500 m increments) and MPOD values of 0.00, 0.10, 0.25, 0.50, and 1.00 were chosen to illustrate a wide range of densities. Additionally, the atmospheric scattering coefficient for all presented results is 2.00, which represents the midpoint between extreme fog (~0.00) and pure Rayleigh scattering (~4.00) as well as being a reasonable real-world value.[4] The model was built in Python v3.6.4 and heavily used the NumPy (v1.14.0) and Pandas (v0.22.0) libraries. Percentage improvement (which in some circumstances was negative) relative to a 0.00 MPOD observer was calculated and plotted in R v3.4.3 from the output files generated by the modeling Python code.

Mathematically, the method used here was equivalent to that previously presented by O'Brien et al.[9] in a photopic-only examination, but the previous presentation relied upon a serial approach using loops to perform calculations for each wavelength while the current version uses NumPy matrix operations to substantially enhance computational efficiency. This enhancement enabled calculations to be performed for a large range of modeled observer MPODs (0.00 to 1.00 in increments of 0.01) and atmospheric scatter constants (0.00 to 4.00 in increments of 0.01), with results being subset and stored to file for conditions of interest. The present approach was taken as a step toward developing the method for future use as an interactive tool or application.

3 Results

The modeled effects of the filtration of MP on WC varied substantially between different target spectra as well as between the photopic and scotopic luminosity functions. In all cases, contrast was negative for all values, which is to be expected for reflective targets, and approaches 0 as distance increases, which is to be expected as more of the target's luminance is scattered and more airlight intrudes into the line of sight (Table 2).

The results of the present modeling effort address only the calculation of the contrast of the reflective target and do not include estimates of visual sensitivity. Previous literature[10] has shown that sensitivity for positive contrast targets (i.e., targets with a luminance higher than the background) can be increased with increased MPOD. It may be noted further that the visual system's sensitivity to contrast may be impacted by nonoptical effects of the MP as discussed by others, for example, Zimmer and Hammond.[11]

When viewing curves of percent WC change (with increases in contrast treated as positive values) versus a 0.00 MPOD, two distinct phenomena appear.

First, for all tested spectra, there is a "cross-over" distance where MPOD shows no impact on luminance contrast. For distances short of the crossover distance, the MP filters enough of the target luminance to cause a net decrease in contrast. After this distance, the MP reduces enough of both the background luminance and the airlight luminance to offset the filtering of the target luminance and thereby create a net increase in contrast (Tables 3 and 4).

Second, the distance at which this cross-over point occurs varies dramatically between different target reflectance spectra and also changes substantially between photopic and scotopic vision. For an ideal blackbody (where there is no target reflectance, a situation in which increasing distance has no impact on target luminance), the cross-over point is at 0 m

Table 2 WC for blackbody target.

	Photopic					Scotopic				
Range (km)	MP 0.00	MP 0.10	MP 0.25	MP 0.50	MP 1.00	MP 0.00	MP 0.10	MP 0.25	MP 0.50	MP 1.00
1	−0.905	−0.906	−0.907	−0.908	−0.908	−0.885	−0.886	−0.888	−0.891	−0.894
5	−0.609	−0.611	−0.614	−0.617	−0.620	−0.545	−0.548	−0.554	−0.562	−0.572
10	−0.373	−0.376	−0.379	−0.382	−0.386	−0.299	−0.303	−0.309	−0.318	−0.329
15	−0.230	−0.232	−0.235	−0.238	−0.241	−0.166	−0.169	−0.174	−0.181	−0.190
20	−0.143	−0.144	−0.146	−0.149	−0.151	−0.092	−0.095	−0.098	−0.104	−0.110
25	−0.089	−0.090	−0.092	−0.093	−0.095	−0.052	−0.053	−0.056	−0.060	−0.064
30	−0.056	−0.057	−0.058	−0.059	−0.060	−0.029	−0.030	−0.032	−0.034	−0.038
35	−0.035	−0.036	−0.036	−0.037	−0.038	−0.017	−0.017	−0.018	−0.020	−0.022
40	−0.022	−0.023	−0.023	−0.024	−0.024	−0.010	−0.010	−0.011	−0.012	−0.013
45	−0.014	−0.014	−0.015	−0.015	−0.015	−0.005	−0.006	−0.006	−0.007	−0.008
50	−0.009	−0.009	−0.009	−0.010	−0.010	−0.003	−0.003	−0.004	−0.004	−0.005

Table 3 WC For OD green nylon webbing target.

	Photopic					Scotopic				
Range (km)	MP 0.00	MP 0.10	MP 0.25	MP 0.50	MP 1.00	MP 0.00	MP 0.10	MP 0.25	MP 0.50	MP 1.00
1	−0.840	−0.840	−0.840	−0.840	−0.841	−0.835	−0.835	−0.835	−0.835	−0.834
5	−0.565	−0.567	−0.569	−0.571	−0.573	−0.514	−0.516	−0.520	−0.526	−0.533
15	−0.346	−0.348	−0.351	−0.354	−0.357	−0.282	−0.285	−0.290	−0.297	−0.306
20	−0.213	−0.215	−0.218	−0.220	−0.223	−0.156	−0.158	−0.163	−0.169	−0.177
25	−0.132	−0.134	−0.136	−0.138	−0.140	−0.087	−0.089	−0.092	−0.097	−0.103
30	−0.082	−0.083	−0.085	−0.086	−0.088	−0.049	−0.050	−0.052	−0.056	−0.060
35	−0.051	−0.052	−0.053	−0.054	−0.056	−0.027	−0.028	−0.030	−0.032	−0.035
40	−0.032	−0.033	−0.034	−0.034	−0.035	−0.016	−0.016	−0.017	−0.019	−0.021
45	−0.020	−0.021	−0.021	−0.022	−0.022	−0.009	−0.009	−0.010	−0.011	−0.012
50	−0.013	−0.013	−0.014	−0.014	−0.014	−0.005	−0.005	−0.006	−0.006	−0.007
55	−0.008	−0.008	−0.009	−0.009	−0.009	−0.003	−0.003	−0.003	−0.004	−0.004

(Fig. 2). For the olive drab nylon webbing spectra tested, the photopic cross-over point is between 0.5 and 1.0 km, but the scotopic cross-over point is between 1.0 and 1.5 km (Fig. 3). With the yellow nylon webbing spectra tested, the photopic cross-over point is between 15.5 and 16 km, but the scotopic cross-over point is between 28.5 and 29 km (Fig. 4).

4 Discussion

The model results suggest that the impact of MP on luminance WC differs between photopic and scotopic vision. For all tested spectra, any contrast enhancement or reduction due to MPOD was of greater magnitude under scotopic conditions than photopic conditions. Considering that the spectral absorption of the MP (Fig. 5) has more overlap with the scotopic sensitivity than with the photopic sensitivity curve (Fig. 6), this is to be expected. Although the original presentation of this model by Wooten and Hammond[4] suggested only improvements in luminance WC from MP, the present model shows that decreases occur under certain circumstances, and that they are likely nontrivial.

Before attempting to use this model to estimate human visual performance, several limitations must be taken into consideration. MP is selectively concentrated in the central fovea,[12] which has maximal cone density and minimal rod density,[13] reducing the impact of MP on scotopic vision. However, there are typically significant levels of MP at

Table 4 WC for yellow nylon webbing target.

	Photopic					Scotopic				
Range (km)	MP 0.00	MP 0.10	MP 0.25	MP 0.50	MP 1.00	MP 0.00	MP 0.10	MP 0.25	MP 0.50	MP 1.00
1	−0.251	−0.246	−0.240	−0.233	−0.227	−0.389	−0.369	−0.339	−0.295	−0.238
5	−0.167	−0.165	−0.162	−0.159	−0.156	−0.229	−0.218	−0.201	−0.177	−0.147
10	−0.101	−0.101	−0.100	−0.099	−0.098	−0.119	−0.114	−0.106	−0.095	−0.081
15	−0.062	−0.062	−0.062	−0.062	−0.062	−0.062	−0.060	−0.056	−0.051	−0.045
20	−0.039	−0.039	−0.039	−0.039	−0.039	−0.033	−0.032	−0.030	−0.028	−0.025
25	−0.024	−0.024	−0.025	−0.025	−0.025	−0.017	−0.017	−0.016	−0.016	−0.014
30	−0.015	−0.015	−0.016	−0.016	−0.016	−0.009	−0.009	−0.009	−0.009	−0.008
35	−0.010	−0.010	−0.010	−0.010	−0.010	−0.005	−0.005	−0.005	−0.005	−0.005
40	−0.006	−0.006	−0.006	−0.007	−0.007	−0.003	−0.003	−0.003	−0.003	−0.003
45	−0.004	−0.004	−0.004	−0.004	−0.004	−0.002	−0.002	−0.002	−0.002	−0.002
50	−0.003	−0.003	−0.003	−0.003	−0.003	−0.001	−0.001	−0.001	−0.001	−0.001

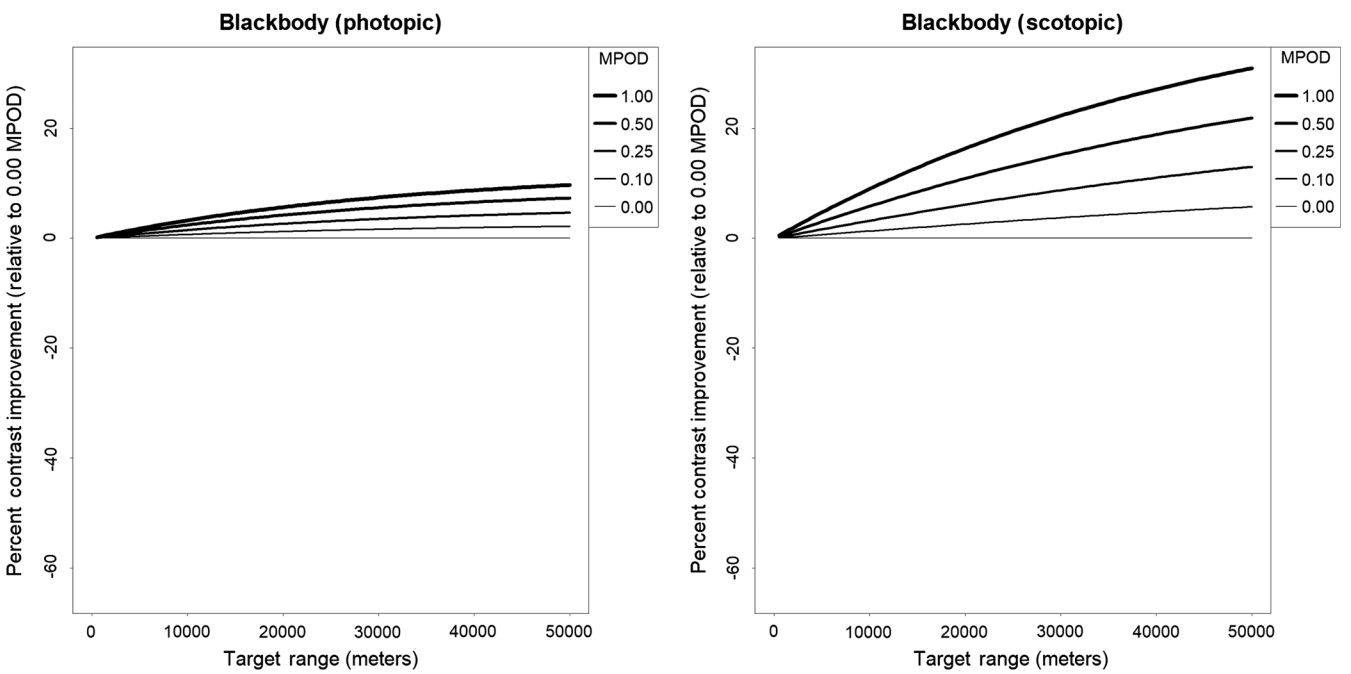

Fig. 2 WC changes for black body target (relative to MP 0.00 observer).

the retinal eccentricities where rod density first exceeds cone density.[14] Additionally, some subjects exhibit atypical spatial distributions of MP[15] and the distribution of MP tends to widen with age,[16] both of which could change the influence of MP on scotopic vision. As true scotopic viewing conditions are rare in outdoor environments, interpolating a mesopic model from the photopic and scotopic models is likely to be more useful in predicting visual performance. It may also be useful to treat photopic sensitivity as sensitivity for each cone type, rather than as a monolithic photopic sensitivity curve, to allow for color contrast to be determined in addition to luminance contrast. Incorporating the nonlinear topography of both the photoreceptor mosaic and the distribution of MP into the presented model would both multiplicatively increase the computational requirements well beyond the equipment currently available to the authors, but down-selection of currently captured variables into constants would permit this for future use.

The current iteration of this modeling effort produces an abundance of data. Modeling 101 MP densities for each of 401 atmospheric scatter constants means that 40501 WC values are calculated for each specified combination of distance,

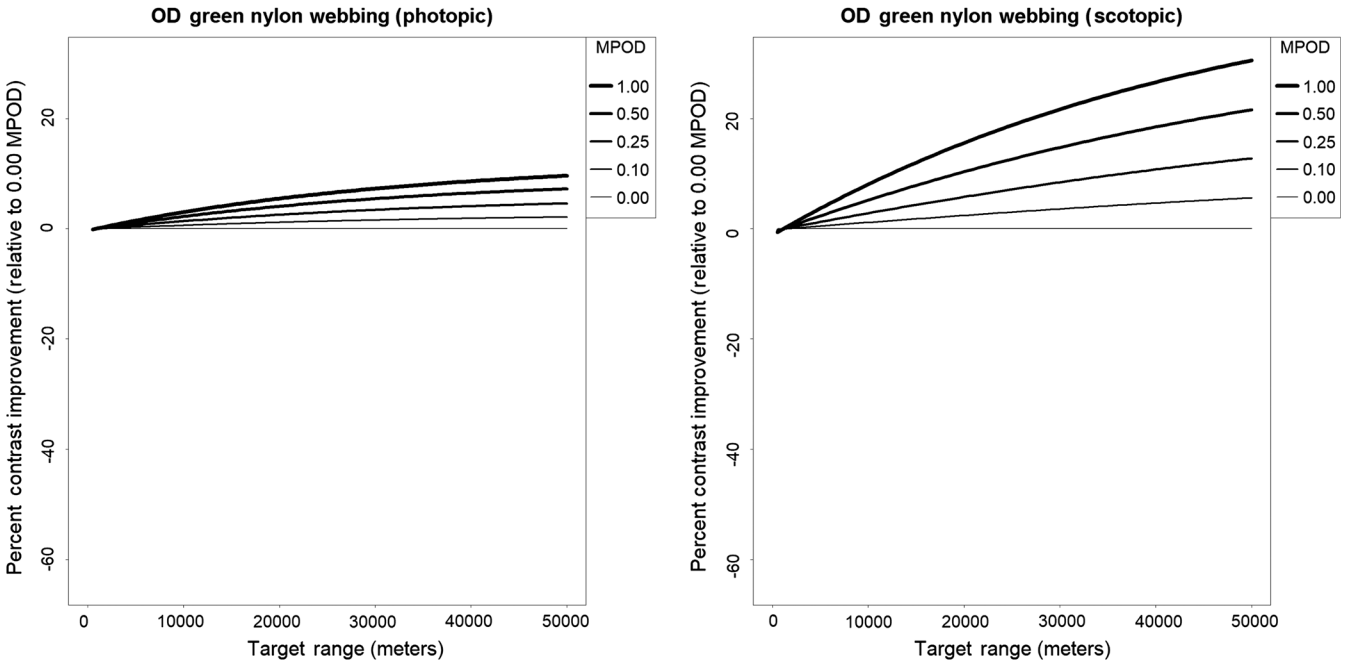

Fig. 3 WC changes for OD green nylon webbing target (relative to MP 0.00 observer).

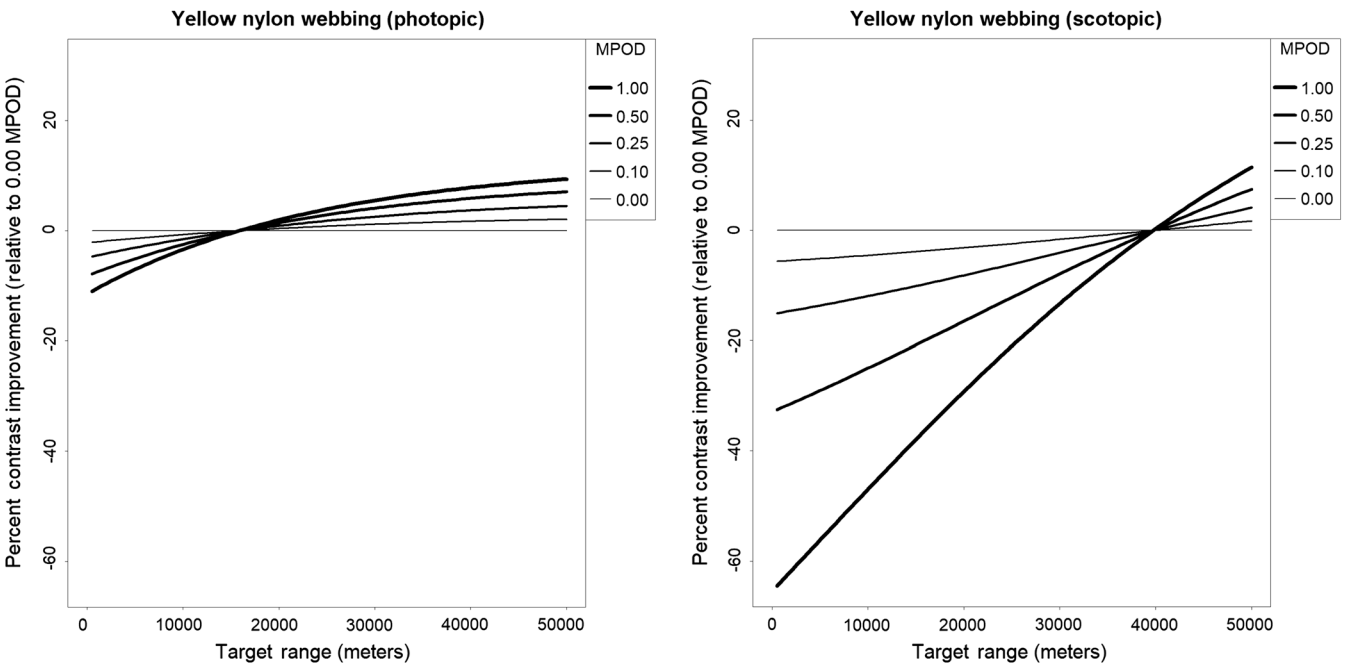

Fig. 4 WC changes for yellow nylon webbing target (relative to MP 0.00 observer).

luminosity function, illuminant spectrum, and target spectrum. The overhead required to produce these calculations precludes the model from use on most current computing systems prior to some sort of subsetting as tabular data or a database. Nonetheless, these output data may have applications in predicting the visibility of targets in aviation and military environments. Because the luminance WC changes with distance toward an asymptote of 0, it may be practical to calculate values for a small number of ranges and fit to the data an exponential decay function or other smooth curve.

Future developments to the model could address mesopic vision, most likely by taking both a photopic and scotopic luminosity function and creating a combined sensitivity curve based on complementary weights as current CIE standards recommend.[17] If filter spectra other than that of MP are substituted, this model may have utility in designing specialized eyewear for aerial or ground observers of aircraft or unmanned aerial vehicles (UAVs). With some streamlining, this code may eventually be useful in optimizing paint and other material selection for UAVs and aircraft to maximize or minimize visual detection at different distances or under

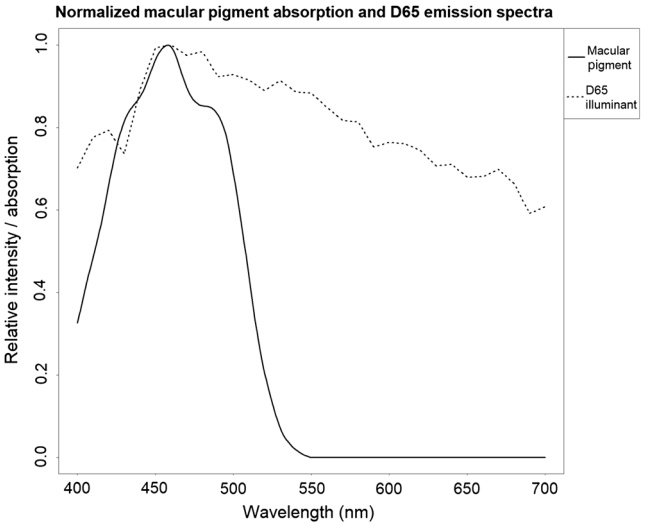

Fig. 5 Spectra of MP and D65 illuminant.

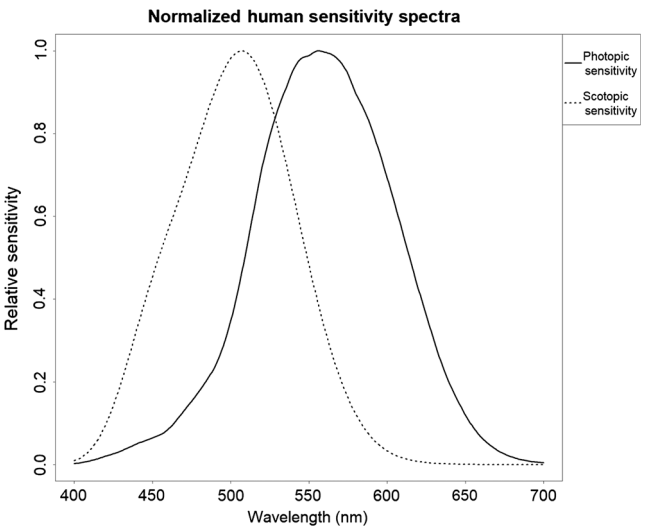

Fig. 6 Photopic and scotopic sensitivity curves.

different atmospheric conditions. It should also be possible to run the model in parallel with the sensitivity data for the separate cone classes to aid in the prediction of chromatic contrast. Additionally, this model serves as a potential starting point in creating a detection probability model for observers viewing distant objects, which would need to incorporate the visual angle of the target as well as overall luminance and other factors.[18]

Acknowledgments

This research was supported by the U.S. Army Medical Research and Materiel Command (USAMRMC): Military Operational Medicine Research Program; Task Area: Aeromedical Standards for Degraded Visual Environment (DVE) Operations and Countermeasures; Research Project: Low contrast sensitivity as a function of macular pigment density and countermeasures. The authors gratefully acknowledge the support, contributions, and help of Ms. Vicky Anderson, Ms. Jessica Cumbee, Ms. Catherine Davis, Ms. Amanda Hayes, and Dr. Thomas Harding. The authors have no relevant financial interests in this manuscript or other potential conflicts of interest to disclose.

References

1. R. A. Bone et al., "Distribution of lutein and zeaxanthin stereoisomers in the human retina," *Exp. Eye Res.* **64**(2), 211–218 (1997).
2. L. Rayleigh, "On the transmission of light through an atmosphere containing small particles in suspension, and on the origin of the blue of the sky," *London Edinburgh Dublin Philos. Mag. J. Sci.* **47**(287), 375–384 (1899).
3. G. Mie, "Beiträge zur optik trüber medien, speziell kolloidaler metallösungen," *Ann. Phys.* **330**(3), 377–445 (1908).
4. B. R. Wooten and B. R. Hammond, "Macular pigment: influences on visual acuity and visibility," *Prog. Retinal Eye Res.* **21**(2), 225–240 (2002).
5. R. A. McClatchey et al., "Optical properties of the atmosphere," Tech. Rep., Air Force Cambridge Research Laboratory, Hanscom AFB, Massachusetts (1972).
6. N. Kopeika, "Spatial-frequency-and wavelength-dependent effects of aerosols on the atmospheric modulation transfer function," *J. Opt. Soc. Am.* **72**(8), 1092–1094 (1982).
7. A. Stockman, http://www.cvrl.org/, Colour and Vision Research Laboratory (6 August 2018).
8. R. F. Kokaly et al., "USGS spectral library version 7," Tech. Rep., US Geological Survey (2017).
9. K. J. O'Brien, L. A. Temme, and P. M. St. Onge, "Modeling the effect of macular pigment enhancement on vision in degraded visual environments (DVE)," *Proc. SPIE* **10642**, 1064204 (2018).
10. J. M. Stringham et al., "Macular pigment and visual performance in low-light conditions," *Invest. Ophthalmol. Visual Sci.* **56**(4), 2459–2468 (2015).
11. J. P. Zimmer and B. R. Hammond Jr., "Possible influences of lutein and zeaxanthin on the developing retina," *Clin. Ophthalmol.* **1**(1), 25–35 (2007).
12. M. Trieschmann et al., "Macular pigment in the human retina: histological evaluation of localization and distribution," *Eye* **22**(1), 132–137 (2008).
13. G. Osterberg, "Topography of the layer of the rods and cones in the human retina," *Acta Ophthalmol.* **13**(6), 1–102 (1935).
14. R. Bone et al., "Analysis of the macular pigment by HPLC: retinal distribution and age study," *Invest. Ophthalmol. Visual Sci.* **29**(6), 843–849 (1988).
15. B. R. Hammond, B. R. Wooten, and D. M. Snodderly, "Individual variations in the spatial profile of human macular pigment," *J. Opt. Soc. Am. A* **14**(6), 1187–1196 (1997).
16. S.-F. Chen, Y. Chang, and J.-C. Wu, "The spatial distribution of macular pigment in humans," *Curr. Eye Res.* **23**(6), 422–434 (2001).
17. C. C. I. de l'Éclairage, "Recommended system for mesopic photometry based on visual performance," CIE 191:2010, CIE Central Bureau, Vienna, Austria (2010).
18. W. Middleton, *Vision through the Atmosphere*, University of Toronto Press, Toronto (1952).

Kevin J. O'Brien is a research psychologist in the United States Army Aeromedical Research Laboratory's Warfighter Performance Group, where he was previously a postdoctoral fellow through the Oak Ridge Institute for Science and Education. He received his BS, MS, and PhD degrees in psychology from the University of Georgia in 2009, 2012, and 2015, respectively.

Leonard A. Temme is a member of United Sates Army Aeromedical Research Laboratory's War Fighter Performance Group. He received his PhD in neuropsychology and his MS degree in mathematical statistics. Prior to joining USAARL, he was with the Naval Aerospace Medical Research Laboratory. He held faculty positions at the Physiology Department, SUNY Buffalo and the Ophthalmology Department University of Kansas, Kansas City. He has published widely in vision, human performance, and aviation.

Paul M. St. Onge is a member of the U.S. Army Aeromedical Research Laboratory, Fort Rucker, AL, in the Warfighter Performance Group, in the Hypoxia Laboratory research team. He graduated from LeMoyne College in Syracuse, NY; Arizona State University, Tempe, AZ; and Auburn University, Auburn, AL with a doctorate in kinesiology.